



Enhanced Antibacterial Activity of Chitosan Nanoparticles Encapsulated in Annatto Seed Extract Against Meat-Borne Bacterial Contamination

Z. H. A. Altaee ^{1*} 

L. A. Alzubaidi ² 

A. M. S. Al-Rubeii ¹

¹ Dept. of Animal Production, College of Agricultural Engineering Sciences, University of Baghdad.

² Research and Technology Center of Environment, Water and Renewable Energy. Scientific Research commission.

***Correspondence to:** Zamzam Hussein Ali. Department of Animal Production, College of Agricultural Engineering Sciences, University of Baghdad, Iraq.

Email: Zamzam.Ali2201p@coagri.uobaghdad.edu.iq

Article info

Received: 2024-12-21

Accepted: 2025-06-26

Published: 2025-12-31

DOI-Crossref:

10.32649/ajas.2025.189371

Cite as:

Altaee, Z. H. A., Alzubaidi, L. A., and Al-Rubeii, A. M. S. (2025). Enhanced Antibacterial Activity of Chitosan Nanoparticles Encapsulated in Annatto Seed Extract Against Meat-Borne Bacterial Contamination. Anbar Journal of Agricultural Sciences, 23(2): 1325-1342.

©Authors, 2025, College of Agriculture, University of Anbar. This is an open-access article under the CC BY 4.0 license

(<http://creativecommons.org/licenses/by/4.0/>).

Abstract

Active compounds from annatto seeds were extracted using alcoholic solvents (ethanol) and synthesized with chitosan nanoparticles (CsNPs) to analyze their properties and antibacterial activity. The annatto seed extracts yielded 4.3% of the powder. The CsNPs were synthesized via ion coagulation which is simple and does not require harsh chemicals. The particle sizes ranged from 39.48 to 43.48 nm. UV-Vis analysis showed an absorption peak at 214 nm for the annatto extract/ chitosan nanoparticles (A Ex/CsNPs), indicating their formation by the surface plasmon resonance (SPR) phenomenon. The presence of functional groups such as alcohols, phenols, and alkaloids in the extract and nanoparticles was confirmed. Heightened intensity of the amide peak of 1580–1650 cm⁻¹ in the nanoparticles was also shown, indicating the interaction of the bioactive compounds with chitosan. The nanoparticles exhibited two peaks at angles of 19.9° and 23.7°, confirming their crystalline structure. Lower peak intensity was observed upon incorporation of the extract, indicating increased flexibility of the polymer chains. Microscopic images revealed nanoparticles of sizes 39.48–43.48 nm with rough surfaces, which may enhance interaction with biological targets. The



alcoholic extract (A Ex) showed activity against bacteria such as *E. coli* and *S. aureus* at a minimum inhibitory concentration (MIC) of 1.17 mg/ml, while the A Ex/CsNPs recorded higher activity of 92.08 µg/ml with three replicates. This activity is attributed to phenolic compounds, flavonoids (antioxidants), and alkaloids that weaken bacterial membranes, and disrupts their cellular functions. It can be concluded that nanoparticles loaded with annatto extract have superior antibacterial activity compared to the crude extract due to their greater stability and surface area. These findings offer new avenues for applications in the pharmaceutical and food industries as natural alternatives to synthetic preservatives.

Keywords: Antibacterial, Annatto extract, Sol-gel, Contaminated fresh meat.

النشاط المضاد للبكتيريا المعزز لجسيمات الكيتوسان النانوية المحملة بمستخلص بذور الأناتو ضد البكتيريا الملوثة للحوم

زمن حسين علي الطائي^{1*}  لبيب احمد الزبيدي² 

¹ قسم الانتاج الحيواني، كلية علوم الهندسة الزراعية، جامعة بغداد، بغداد، العراق.

² مركز البحوث والتكنولوجيا البيئية والمياه والطاقة المتعددة، هيئة البحث العلمي.

*المراسلة الى: زمن حسين علي الطائي، قسم الانتاج الحيواني، كلية علوم الهندسة الزراعية، جامعة بغداد، بغداد، العراق.

البريد الإلكتروني: Zamzam.Ali2201p@coagri.uobaghdad.edu.iq

الخلاصة

تناولت الدراسة استخلاص المركبات الفعالة من بذور الأناتو باستخدام المذيبات الكحولية (الإيثانول)، وتخليق دفائق الكيتوسان النانوية (CsNPs) المحملة بالمستخلص، وتحليل خصائصها وتقدير فعاليتها المضادة للبكتيريا. حقق الاستخلاص الكحولي لبذور الأناتو نسبة 4.3% من المسحوق. تم تخليق دفائق الكيتوسان النانوية (CsNPs) بطريقة التخثر الأيوني، وهي طريقة بسيطة لا تتطلب مواد كيميائية قاسية. تراوحت أحجام الدفائق بين 39.48 و43.48 نانومتر. أظهر تحليل الأشعة فوق البنفسجية- المرئية ذروة امتصاص عند طول موجي 214 نانومتر لمستخلص الأناتو/ دفائق الكيتوسان النانوية (A Ex/ CsNPs)، مما يشير إلى تكوينها بواسطة ظاهرة رنين البلازمون السطحي (SPR)، تم تأكيد وجود مجموعات وظيفية مثل الكحولات والفينولات والقلويات في المستخلص والدفائق النانوية. كما ظهر زيادة في شدة ذروة الأميد (1580-1650) سم⁻¹ في الدفائق النانوية، مما يشير إلى تفاعل المركبات الفعالة بيولوجيًا مع الكيتوسان. أظهرت الدفائق النانوية قمتين بزرويا

19.9 درجة و 23.7 درجة، مما يؤكد بنيتها البليورية. لوحظ انخفاض في شدة الذرة عند دمج المستخلص، مما يشير إلى زيادة مرونة سلاسل البوليمر. كشفت الصور المجهرية عن دقائق نانوية بحجم 43.48-39.48 نانومتر ذات أسطح خشنة، مما قد يعزز التفاعل مع الأهداف البيولوجية. أظهر المستخلص الكحولي (A Ex) نشاطاً ضد البكتيريا مثل *Staphylococcus aureus* و *Escherichia coli* بتركيز مثبط أدنى (MIC) يبلغ 1.17 ملغم/مل، بينما سجلت الدقائق النانوية (A Ex/ CsNPs) نشاطاً أعلى بلغ 92.08 ميكروغرام/ مل وبثلاث مكررات. يُعزى هذا النشاط إلى المركبات الفينولية والفلافونويدات (مضادات الأكسدة) والقلويات التي تُضعف الأغشية البكتيرية وتعطل وظائفها الخلوية؛ لذلك، يمكننا الاستنتاج أن الدقائق النانوية المُحملة بمستخلص الأناتو تُبدي فعالية مضادة للبكتيريا يفوق المستخلص الخام، نظراً لزيادة ثباتها ومساحة سطحها. تفتح هذه النتائج آفاقاً جديدة للتطبيقات في الصناعات الدوائية والغذائية كبدائل طبيعية للمواد الحافظة الصناعية.

كلمات مفتاحية: تضاد البكتيريا، مستخلص الأناتو، الهمام السائل، لحوم.

Introduction

Microbial contamination in meat primarily occurs on the surface, often originating from animal hides, feces, and intestinal spillage during slaughter and processing (35). Contamination risks also arise from equipment, personnel, pests, and improper storage or transportation conditions (12). Factors influencing microbial presence include the physiological state of the animal, processing hygiene, storage temperatures, and competing microorganisms (21). Preservation methods like refrigeration, drying, irradiation, antimicrobial additives, and modified atmosphere packaging are used to control contamination, with the aim of ensuring safety, extending shelf life, and maintaining meat quality by inhibiting microbial growth (26). Annatto seeds (*Bixa orellana* L.) are used as a natural colorant in the meat industry, ranking second in economic importance worldwide among all natural colorants, and their extract exhibits antimicrobial and antioxidant properties (36).

The seeds display yellow-red pigments and reduce microbial spoilage in meat products (32). Thin (1–100 nm), layer-by-layer antimicrobial coatings inhibit pathogen growth, which is crucial for anaerobic-packed meats to maintain sensory quality (5). The European Food Safety Authority indicates that nanotechnology can significantly enhance food packaging, and that meat quality preservation is significantly enhanced by appropriate packaging under optimal storage conditions (12). Some researchers have been developing packaging methods that exclude artificial chemicals; this advancement may assist in managing odor and lipid oxidation, thereby inhibiting microbial growth (2). The objectives of this research were to biosynthesize and characterize chitosan nanoparticles encapsulated with annatto extract to evaluate their enhanced antimicrobial efficacy against meat contaminants as against using annatto alone. This approach merges natural compounds with advanced nanotechnology to obtain safer, longer-lasting meat products.

Materials and Methods

Preparation of annatto alcoholic extract (A Ex): The annatto seed powder (150 g) was extracted and dried in an electric oven. Alcoholic extraction (85% ethanol, 750 ml) was performed for 8 h using a Soxhlet apparatus. The extract was concentrated using a rotary evaporator and dried in an electric oven at 40-45 °C. The extract yield was calculated using the Eq. (3).

$$\% \text{ Extract Yield (g/100 g)} = W1/W2 * 100$$

where, W2 is the weight of the dried plant powder, and W1 the weight of the extract residue after solvent removal.

Nanoparticle biosynthesis: This paper details the methodology for developing chitosan nanoparticles encapsulated with annatto extract (A Ex/CsNPs) to enhance antimicrobial activity in meat preservation. The key steps included:

- A. Chitosan-A Ex adduct formed using a Dean-Stark apparatus: Chitosan (5%) and annatto extract (1%) were mixed in equimolar ratios, and the condensation occurred in the presence of xylene using the Dean-Stark apparatus until the theoretical water quantity was separated. The resulting chitosan amide product was sequentially filtered and washed several times with methanol, hot distilled water, and ethanol, and then dried (1).
- B. Ionic gelation with tripolyphosphate (TPP) creates A Ex/CsNPs: Chitosan nanoparticles loaded with annatto extract (A Ex/CsNPs) were synthesized using an ionic gelation method. The Cs-A Ex adduct was dissolved in acetic acid, and tripolyphosphate (TPP) was added at a 1:2.5 ratio. The mixture was stirred for 6 h at room temperature, leading to the formation of NPs. The nanoparticles were separated, washed, and dried (27).

Overall, the process involved creating a chitosan-annatto extract adduct followed by the formation of nanoparticles through ionic gelation.

- C. Characterization of annatto ex/chitosan nanoparticles (5): This study utilized advanced analytical techniques to characterize chitosan nanoparticles loaded with annatto seed extract.
 1. UV-Vis Spectroscopy: Absorption spectra (200–800 nm) were measured using a dual-beam system in a 1 cm quartz cell, with distilled deionized water as a control. The concentrated samples were diluted 1:10 (2). Measurements were conducted at the Scientific Research Commission, Research and Technology Center of the Environment, Water and Renewable Energy Department, Iraq.
 2. FTIR Analysis: Functional groups were identified using Shimadzu FTIR (4000–400 cm^{-1} range, 4 cm^{-1} resolution). The samples were prepared as potassium bromide (KBr) pellets (1:99 sample-to-KBr ratio) following (2). Analyses were performed at the Scientific Research Commission, Research and Technology Center of the Environment, Water and Renewable Energy Department, Iraq.
 3. AFM, SEM, EDX: Assessments of morphology and elemental composition were done according to (17).
 4. XRD: This was done to determine crystal structure and particle size, and performed according to Eq. (29).

Collaboration: Analyses were conducted at institutions in Iraq and Iran. This study aimed to optimize a natural, nanotechnology-based solution for inhibiting microbial contamination in meat products.

This research focused on the methodical preparation and characterization of nanoparticles, leveraging standardized protocols and institutional collaboration to ensure accuracy. The measurements were performed at the Scientific Research Commission, Research and Technology Center of the Environment, Water and Renewable Energy Department, Iraq.

5. Determination of the minimum inhibition concentration of annatto seed extract and its nanoparticles.

The study evaluated the antibacterial activity of chitosan nanoparticles loaded with annatto seed extract against *Salmonella* spp., *E. coli*, *Staphylococcus* spp., and *Pseudomonas* spp. The microtiter plate (MTP) method was used to determine MBC and minimum inhibitory concentrations (MIC). Key steps included:

- Preparation: serial dilutions of nanoparticles (annatto seed extract: 2.3–1209 µg/ml) in a 96-well plate.
- Controls: Well 11 (Mueller Hinton broth) and, Well 12 (bacterial suspension).
- Bacterial inoculation: 1.5×10^8 CFU/mL (McFarland 0.5 standard).
- Incubation: Plates were incubated at 37 °C for 24 hours. Resazurin (0.015%) was added post-incubation; and the color change was monitored after 2–4 h.
- Results Interpretation: MIC: Last well retained blue color (no bacterial growth).
- Sub-MIC (SIC): first pink well (indicating partial inhibition).

The method, adapted from (9), provided a systematic approach to assess antimicrobial efficacy, leveraging resazurin as a metabolic activity indicator.

Results and Discussion

Extraction in the pharmaceutical field separates the medicinally active parts of plant or animal tissues, such as alkaloids, flavonoids, terpenes, saponins, steroids, and glycosides, from the inactive or inert parts using special solvents in standard extraction procedures. Plant products formed through this are mostly dirty liquids, semisolids, or powders that are only meant to be taken orally or applied to the skin. Medicinal plants are collected and handled so that they could be used directly as herbal or traditional medicine or in experiments (16).

The alcoholic (ethanolic) extraction to yield phytochemicals from annatto seeds resulted in a satisfactory yield of 4.3% annatto seeds powder (Fig. 1).

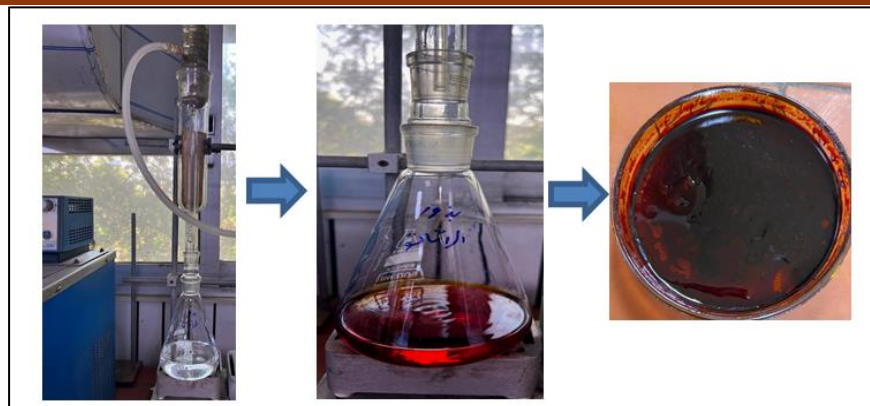


Figure 1: Annatto seeds extraction process (Soxhlet alcoholic extraction).

Annatto seeds alcoholic extract/chitosan nanoencapsulation biosynthesis: The alcoholic extract of annatto seeds has shown promising results in the production of chitosan nanoparticles (CNP). Due to changes in its molecular structure during manufacture, chitosan is no longer soluble in acid solutions and can exist in gel-like or liquid forms (31) (Fig. 1).



Figure 2: A Ex/Chitosan nanoencapsulation biosynthesis process.

Natural chitosan (Cs) is a complex carbohydrate that is positively charged and is made when chitin is deacetylated. Cs is good material for developing nanocarrier systems because it breaks down naturally, is sensitive to pH, and is easy chemically (33). There are other ways to prepare chitosan nanoparticles, but ionic gelation is usually the most common because it can be used in many situations. The method is simple and straightforward, and improves the specific actions of the chemicals inside. (26). It produces chitosan nanoparticles with sizes between 125 and 175 nm.

Characterization of annatto extract/chitosan nanoparticles: UV-Vis spectroscopy was performed at different wavelengths after dilution with deionized water to obtain a good absorption value. The presence of broad resonances in the UV-Vis absorption spectra of annatto extract/chitosan encapsulated nanoparticles obtained from UV-Vis analysis indicates the formation of encapsulated nanoparticles in the solution (3). The existence of an absorption peak at about 275, 240.5, and 209 nm in Ex A indicated absorbance at 1.234, 0.526 and 0.499. Meanwhile, while the maximum absorption peak at approximately 214 nm in the A Ex/CsNPs indicated nanoparticle formation due to surface plasmon resonance (SPR) electrons on the surface of the nanoparticles, and the differences in the wavelength peak and absorbance comparison with UV-Vis spectra of A Ex. The SPR pattern is determined

by the parameters of the individual particles, such as size and shape, as well as the dielectric properties of the synthesis media and interactions between nanoparticles. The strength of the SPR band increased with interaction time, indicating that chitosan nanoparticles were synthesized (25).

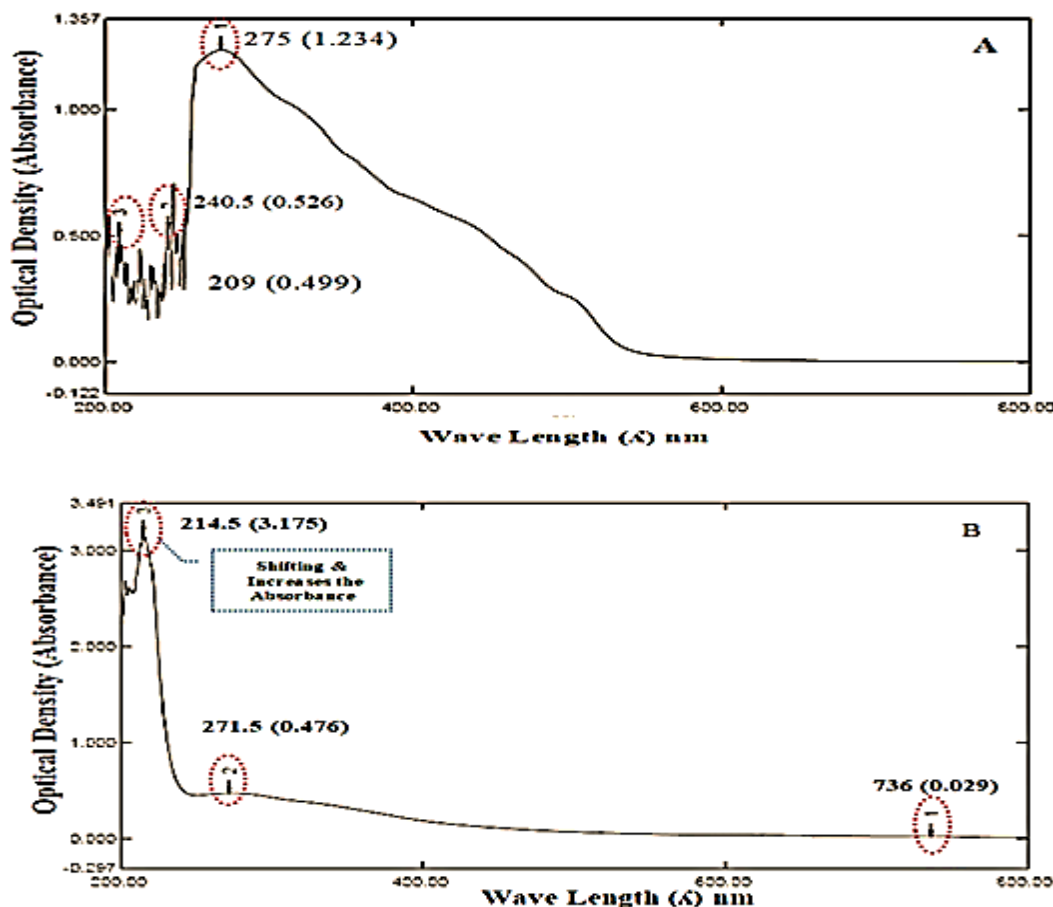


Figure 3: Uv-Vis Spectroscopy of (A) Annatto alcoholic extract–A Ex and (B) A Ex/ CsNPs.

FTIR of A Ex and A Ex/CsNPs: Both the A Ex and the biosynthesized A Ex CsNPs may be seen in the FTIR spectra presented in Table 1. Fig. 4A shows the A Ex spectra containing peaks indicative of different biomolecules, such as alcohol and phenol (3610-3640) cm^{-1} . The predicted chemical makeup of A Ex and chitosan molecules agrees with these findings. Fig. 4B shows that the spectra of biosynthesized nanoencapsulated particles are very close to the A Ex spectrum, indicating that the biomolecules from the extract were successfully attached to the surfaces of the nanoparticles. Water molecules, phenol, terpenoids, and flavonoids are all examples of biomolecules that may be involved. The detected peaks may also be attributable to leftover O-H groups which are products of the synthesis process.

Table 1 provides an exhaustive list of the recognized functional categories together with the corresponding wavenumbers. The disparity in intensity between the A Ex/CsNPs spectra and the amide I peak (1580-1650) is an important finding. An increase the intensity of the nanoparticles' spectra indicates that their associated amide content is higher. This may be explained by the fact that several biomolecules attach to the material during synthesis, which may serve as a stabilizing factor. The

absence of many peaks in the nanoparticle spectrum may be attributed to attachment sites with chitosan and tripolyphosphate compounds. The presence of many indicators of different active compounds, including alkaloids, phenols, and terpenoids, can indicate the efficiency of the nano-encapsulation process and its association with chitosan and polyphosphate triphosphate.

This result is reinforced by the analysis of the presence of carbon and oxygen, confirming the presence of chitosan and other elements such as phosphorus, sodium, and potassium (4C). (29) found that biosynthesis-encapsulated nanoparticles containing A Ex and chitosan molecules had attachment sites not filled in by A Ex/CsNPs (665-910, 2312.65, 2434.17 cm⁻¹). The H-C=O and C-H stretch at 2695-2830 cm⁻¹ revealed structural details of chitosan. FTIR analysis, which is performed alongside the bioconversion of chitosan nanoparticles, conformed the structural stability of chitosan.

Table 1: Results of the FTIR analysis of A Ex and A Ex/CsNPs.

Annatto Extract Functional Groups. cm ⁻¹	Description	A Ex/CsNPs. cm ⁻¹
532.35 C-Br stretch	Alkyl halides	553.97 Higher intensity than the annatto extract suggests a higher concentration of alkyl halides compound (saponin, coumarin, terpenoid) groups.
(700-610) 624.94 -C=C-H: C-H bend	Alkynes	624.94 cm ⁻¹ Referred to contain the chitosan molecules
(665-910) cm ⁻¹ 723.31, 835.18 N-H wag	1', 2' amines	Absent
(1000- 650) cm ⁻¹ 997.2 =C-H bend	Alkenes	999.13 cm ⁻¹ Referred to contain the chitosan molecules
1250- 1020 1134.14 C-N stretch	Aliphatic amines	1139.93 cm ⁻¹ Likely due to C-N stretching in alkaloids, possibly from encapsulated biomolecule (phenolic, flavonic, terpenoids, alkaloids) compounds and with higher intensity than Extract because biosynthesis nanoparticles have higher surface structure with smaller sized particles.
1382.96 C-H rock, P=O, C-F, C-O, C -OH	Alkanes	1386.82 Likely due to C-OH stretching in alcohols, esters, and ethers, possibly from encapsulated biomolecules (phenolic, flavonic, terpenoids, Alkaloids) compounds and with higher intensity than Extract because biosynthesis nanoparticles with higher surface structure with the smaller sized particles.
1580- 1650 1641.42 N-H bend	1' amines	1633.714 Higher intensity than the annatto extract suggests higher concentration compound (saponin, alkaloids, phenol) groups.
(2260- 2210) 2312.65 and2434.17 C-N stretch	Nitriles	2695-2830 2879.72 Shifting and finding aldehyde group with H-C=O: C-H stretch. It may be the site of reaction and attachment between the chitosan molecule and the active compound of annatto extract used in biosynthesis nanoencapsulation particles.
3200-3500 3433.29 O-H stretch, H-bonded	Alcohols, phenols	3435.22 Likely due to O-H stretching and H-bonded in alcohols, phenol, possibly from encapsulated biomolecules (phenolic, flavonic, terpenoids, alkaloid) compounds
3610-3640 3739.97 O-H stretch	Alcohols, phenols	3736.12 Likely due to O-H stretching and H-bonded in alcohols, phenol, possibly from encapsulated biomolecules (phenolic, flavonic, terpenoids) compounds and chitosan molecules.

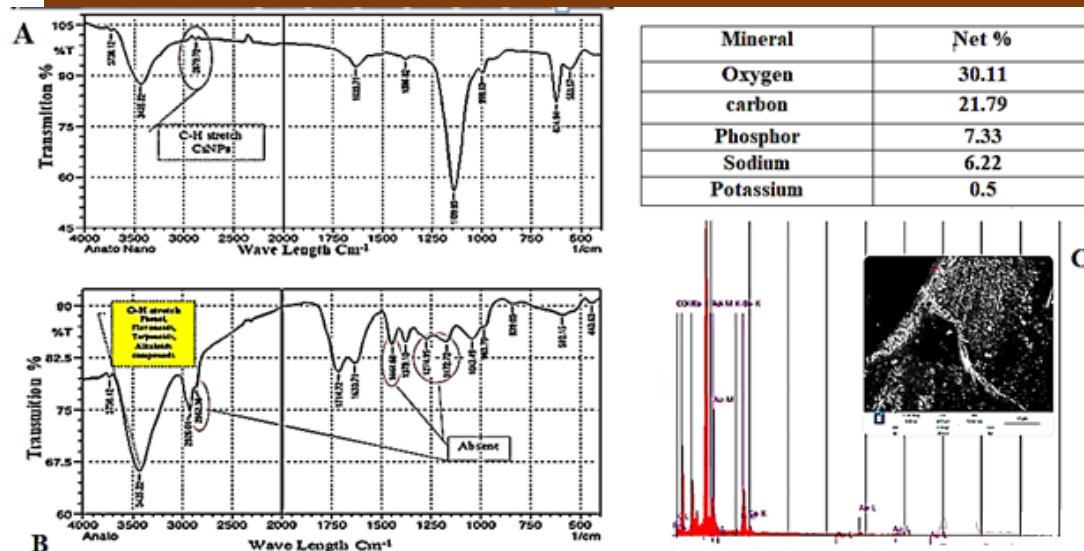


Figure 4: FTIR spectroscopy and EDX(C) of A- A Ex and B- A Ex/CsNPs.

Fe-scanning electron microscope and force electronic microscope analysis of A Ex/CsNPs: Biosynthesized A Ex/CsNPs AFM testing results. The photo shows much shape variability in the nanoparticles which are sized 39.48 - 43.48 nm and having both smooth and rough surface protrusions, lending credence to their high stability. Rough surfaces may provide more extensive interaction between biological processes, such as plant active groups and their targets than smoother surfaces with smaller contact areas (Fig. 5A). Surface protrusions are approximately 83.17 nm, whereas particles typically measure 38.43 nm in height. Fig. 5B shows the nanoparticle aggregates having several sharp edges in addition to their elongated shape and parallel plates. The sharp edges may enhance antibacterial activity by causing damage to bacterial membranes.

Particle analysis conducted with Image J 19 software indicated an average size of 83.17 nm which is consistent with the results derived from AFM analysis. Handling the samples before examination could explain the presence of specific nanoparticle clumps. This offers compelling proof that the particles remain stable and highly effective within the cells. A previous study (33) utilized AFM to examine clove extract loaded with CsNPs; their 3D pictures revealed a homogeneous population of particles with regular surfaces, which was supported by this study's results. AFM imaging showed clove-loaded chitosan nanoparticles interacting intelligently with one another, forming unique aggregates.

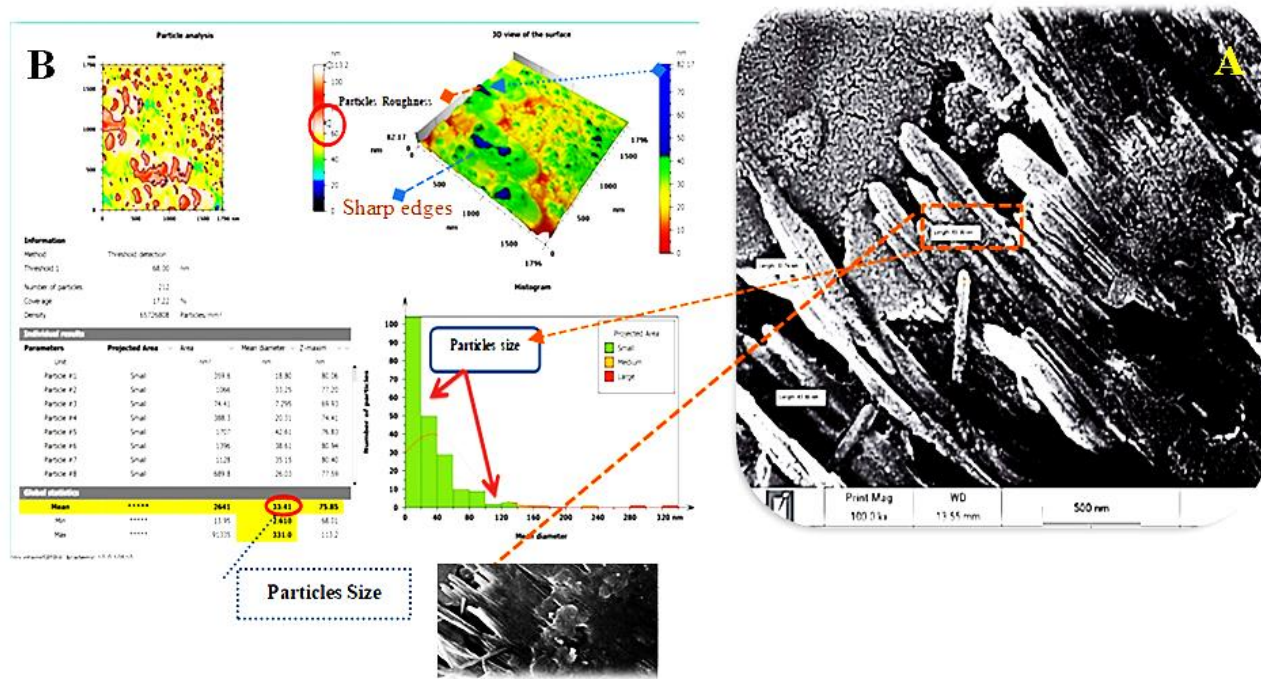


Figure 5: SEM image and AFM results of A Ex/CsNPs X-ray Diffraction-XRD of A Ex/CsNPs.

The attenuated peaks observed in the A Ex/CsNPs pattern signify a reduction in their strength. The reflection of crystal planes results in the formation of X-ray diffraction (XRD) peaks. Figure 6 presents the XRD patterns of the A Ex/CsNPs and natural chitosan. Two distinct peaks at $2\theta = 19.9^\circ$ and 23.7346° (Fig. 6 A) corresponding to the typical chitosan peaks identified in XRD pattern of chitosan nanoparticles (CsNPs) demonstrate that chitosan possesses a well-organized crystal structure. Identifying additional peaks at $2\theta = 18.58^\circ$ for chitosan reduced peak intensity in this study. The XRD pattern of chitosan nanocomposite membranes containing A Ex/CsNPs showed reduced peak intensity (Fig6). The additional diffraction peaks identified in the chitosan nanocomposite membranes reinforced with A Ex/CsNPs correspond to their (1 0 0), (0 0 2), (1 0 1), (1 1 0), and (1 1 2) planes (Fig. 6).

The data demonstrate that the nanocomposite membranes successfully integrated the A Ex nanoparticles which altered the arrangement of polymer chains by affecting the steric interactions and intermolecular hydrogen bonding. (23) demonstrated that incorporating A ex nanoparticles into chitosan resulted in a reduction in the crystallinity of the composite membranes and increased the flexibility of the polymer chains. The results align with the findings of (21), both of which reported a 2θ value of 18.41° .

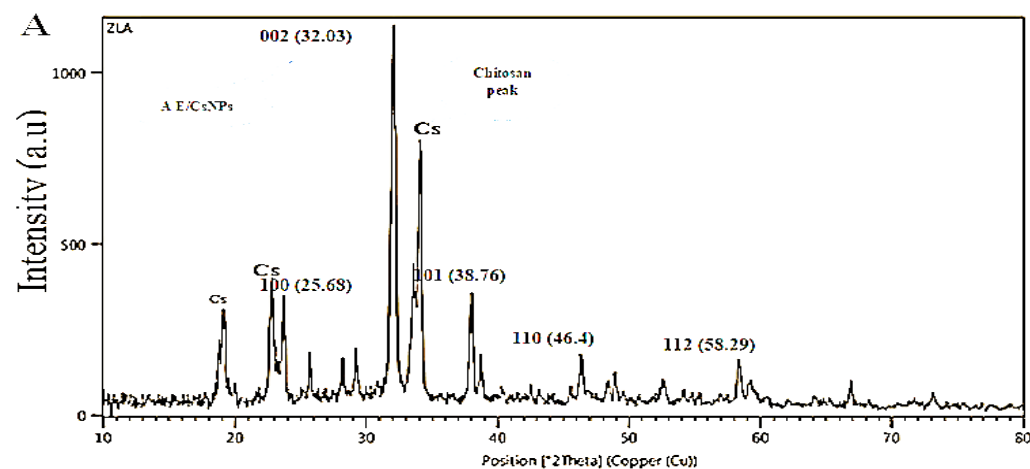


Figure 6: XRD diagram of A Ex/CsNPs.

Total phenolic content of A Ex and A E/CsNPs: Phenolic compounds are major constituents of plants, possessing redox properties that confer antioxidant activity, primarily due to the presence of hydroxyl groups, which facilitate free radical scavenging (22).

The total phenolic content of the annatto seeds extract was evaluated using a straight-line equation (Fig. 7) derived from the absorbance of standard gallic acid at different concentrations, expressed in mg/100 g dry weight. The data in Table 2 indicate that the plant extract (A Ex) had the highest total phenolic content, at 119.7 mg/100 g of plant dry weight, while A Ex/CsNPs recorded 78.5 mg/100 g of plant dry weight.

The total concentration of flavonoids in the alcoholic extract of annatto seeds was 83.5 mg/100 g (Table 2). The concentration was 42.1 mg/ 100 g of plant dry weight in A Ex/CsNPs, based on the straight-line equation of standard rutin absorbance at different concentrations (Fig. 8). Studies by (16) using a gallic acid calibration curve found total phenolic content to be about 52 mg GAE/g of dried extract while total flavonoid content using a rutin calibration curve was about 41 mg rutin/g of dried extract. In contrast, (7 and 14) showed that the highest levels of total phenol (2.87 mg GE/ ml) were produced by extraction using distilled water.

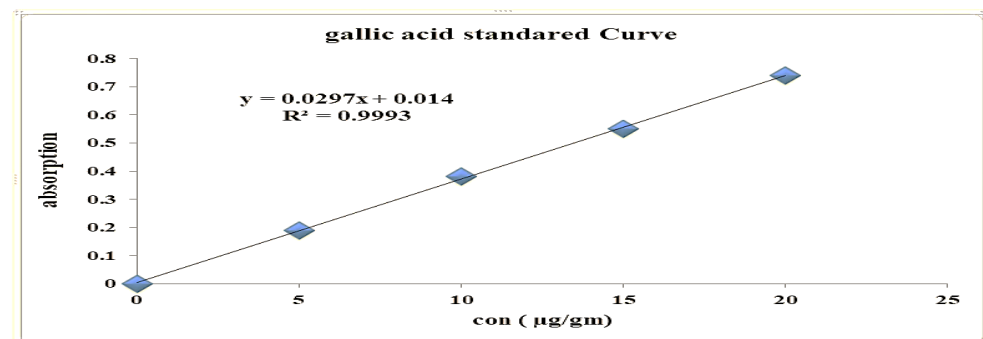


Figure 7: Standard gallic acid calibration curve.

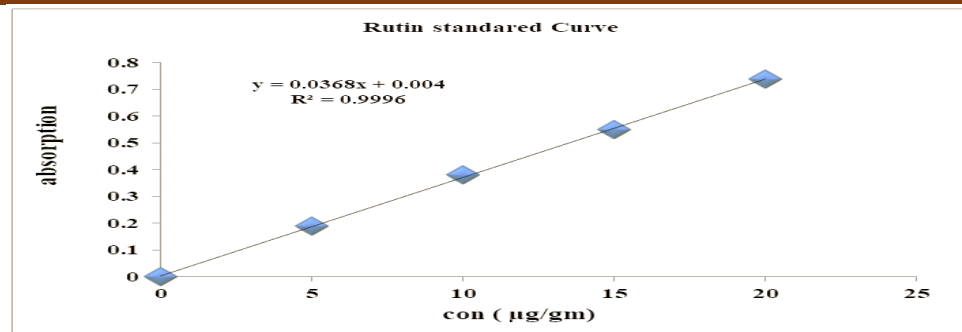


Figure 8: Standard rutin absorbance at different concentrations.

Antibacterial activity determination of A Ex and A Ex/CsNPs: The antibacterial activity of A Ex and A Ex/CsNPs was examined against the *E. coli*, *S. aureus*, *Sal. typhimurium*, and *P. aeruginosa* bacterial isolates. The MIC and sub-MIC ranges of A Ex were 1.17 mg/ml and 0.585 mg/ml, respectively while those for A Ex/CsNPs were 92.08 μg/ml and 46.4 μg/ml, respectively, as shown in Table 2 and Fig. 9.

Table 2: MIC and Sub-MIC of annatto seed extracts against four bacterial isolates.

Isolate No.	CHE (mg/ml)		CHCs-NPs (mg/ml)	
	MIC	Sub-MIC	MIC	Sub- MIC
<i>E. coli</i>	1.17	0.585	92.8	46.4
<i>S. aureus</i>	1.17	0.585	92.8	46.4
<i>Sal. Typhimurium</i>	1.17	0.585	92.8	46.4
<i>P. aeruginosa</i>	1.17	0.585	92.8	46.4

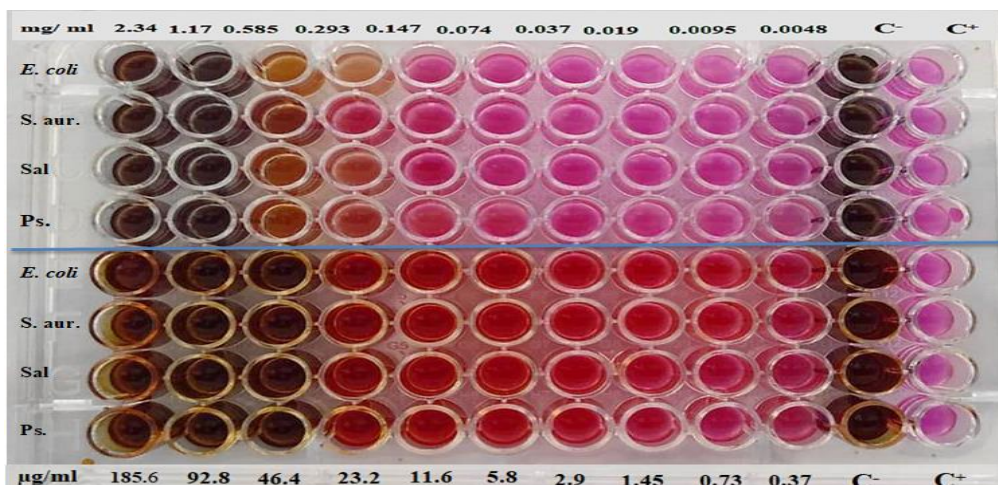


Figure 9: MIC detection by microtiter plate technique of A Ex. and A Ex/CsNPs.

The broth microtiter plate method was employed in a previous study by (33) to determine the effectiveness of niacin and annatto leaf and seed extracts as bacteriostats against gram-positive and gram-negative bacteria. Both *P. aeruginosa* and *B. cereus* had MICs of 512 and 4096 mg/ml, respectively, when tested with annatto extract. For *P. aeruginosa*, *B. cereus*, *L. innocua*, and *A. hydrophila*, the MIC values were 1024, 256, 512, and 256 mg/ ml, respectively, when compared to niacin, the only bacteriocin generally recognized as a natural food preservative. The limit of detection for annatto seeds Ex-ASE in *P. aeruginosa* was 128 mg/ ml and 1024 mg/ml for *B. cereus*. As with annatto leaf extract (ALEx), the concentration ranges

examined for AS Ex did not limit the development of *L.innocua* and *A. hydrophila*. The antibacterial activities of both annatto extracts against *P. aeruginosa* were higher than that of niacin.

Despite extensive evidence of these effects, little is known about the MIC values for the antibacterial effects of annatto extracts. There was antibacterial action against *S. aureus* with MICs of 62.5 mg/ml in ethanolic annatto leaf extracts according to (11) who found that commercial annatto extracts exhibited antibacterial activity against various gram-positive bacteria. Specifically, the extracts were effective against *B. cereus*, *C. perfringens*, and *S. aureus*, with MIC values of 0.08, 0.31, and 0.16% (v/v), respectively. The ethanolic extracts of *B. orellana* leaves and seeds showed activity against all gram-positive and gram-negative bacteria as well as the yeast-like fungus *Candida albicans*, according to (8), with the leaf extract activity being more noticeable. Compared to annatto L. Ex, this investigation demonstrated that annatto stem Ex significantly inhibited bacterial growth.

Antimicrobial properties including phenolic acids, flavonoids, and carotenoids have been found in the active components of the plant. Phenolic rings are toxic to microbes and are the building blocks of some of the most basic phytochemicals with biological activity. Some factors contribute to the observed variation in the antibacterial activity of different plant extracts when tested against different bacterial strains. These include differences in extraction methods, environmental factors (such as soil, humidity, temperature, and climate), physiological variations (such as plant life cycles, growth phase, and stress conditions), and genotype. However, the results show a few bioactive compounds in the ethanolic extract of annatto seeds that are pharmaceutically relevant and may have antibacterial properties. In contrast, it was found by (10) that compared to antibiotics alone, the effects of chitosan and alginate NPs loaded with doxycycline antibiotics increased against MDR *Proteus mirabilis*, *E. coli*, and *E. Faecalis*. According to (16), a plant extract encapsulated with nano-chitosan showed improved effectiveness, even when used with nano-chitosan-loaded NPK fertilizer.

The effects on all aspects of vegetative development were particularly striking when green tea and nettle leaf extract were combined. For instance, antibacterial agents tend to degrade cellular membranes, form complexes with metal ions, harm microbial genetic material, cause cell contents to leak out, inhibit metabolic enzymes, and deplete cellular energy in the form of ATP (27). Several factors influence the bacteriostatic effects of these naturally occurring active substances. These include the chemical properties of the substances, the microorganisms they target, environmental factors such as pH, ionic strength, water activity, temperature, and atmospheric composition, and food properties such as ingredients and initial bacterial load (24).

The cytoplasmic membrane is where the A Ex and A Ex/ Cs NP components are mostly targeted. Owing to their acidic nature, tannin-rich plants can combine with polypeptides to produce powerful water-soluble compounds, giving them antibacterial characteristics. Therefore, these chemicals can effectively destroy bacteria by penetrating their cell walls (4). Flavonoids have antimicrobial and spasmolytic characteristics (14), making them a subclass of polyphenols. According to (27), plant alkaloids are frequently shown to have antibacterial activities.

Conclusions

Nanoencapsulation of annatto extract in chitosan improves antibacterial performance, possibly due to their enhanced stability, targeted delivery, and nanoparticle-bacteria interactions. While the phytochemical content decreased post-encapsulation, the trade-off in efficacy highlights the potential of CsNPs as carriers for bioactive compounds. Further optimization could address the encapsulation efficiency and evaluate in vivo applications. This study underscored the potential of nanotechnology for enhancing herbal extracts for pharmaceutical applications.

Supplementary Materials:

No Supplementary Materials.

Author Contributions:

Zamzam Hussein Ali Altaee: methodology, writing—original draft preparation; Labeeb Ahmed Alzubaidi and Amera Mohammed Saleh Al-Rubeii: writing—review and editing. All authors have read and agreed to the published version of the manuscript.

Funding:

This research received no external funding.

Institutional Review Board Statement:

The study was conducted following the rules of the Iraqi Ministry of Higher Education and Scientific Research, and approved by the Scientific Research Ethics Committee at the University of Baghdad, Iraq and the Research and Technology Center of Environment, Water and Renewable Energy Department.

Informed Consent Statement:

Not applicable.

Data Availability Statement:

Data available upon request.

Conflicts of Interest:

The authors declare no conflict of interest.

Acknowledgments:

The authors extend their sincere thanks to the Deanship of the College of Agricultural Engineering Sciences, University of Baghdad, especially the Department of Animal Production, and the Director of the Department of the Center for Environmental, Water and Renewable Energy Research and Technology for their assistance.

Disclaimer/Journal's Note:

The statements, opinions, and data contained in all publications are solely those of the individual author(s) and contributor(s) and not of AJAS and/or the editor(s). AJAS and/or the editor(s) disclaim responsibility for any injury to people or property resulting from any ideas, methods, instructions, or products referred to in the content.

References

1. Abd El-Ghaffar, M. A., and Hashem, M. S. (2010). Chitosan and its amino acids condensation adducts as reactive natural polymer supports for cellulase immobilization. *Carbohydrate Polymers*, 81(3): 507-516.
<https://doi.org/10.1016/j.carbpol.2010.02.025>.

2. Al-Azzami, A. A., and Mohammed, T. T. (2025). Investigation on Chemical Composition of the Lemongrass Herb and Its Effect on Antimicrobial Activities. *Journal of Life Science and Applied Research*, 6(1). https://doi.10.4103/JLSAR.JLSAR_5_25.
3. Alameri, M. M., Kong, A. S. Y., Aljaafari, M. N., Ali, H. A., Eid, K., Sallagi, M. A., ... and Lai, K. S. (2023). Aflatoxin contamination: An overview on health issues, detection and management strategies. *Toxins*, 15(4): 246. <https://doi.org/10.3390/toxins15040246>.
4. Alamgir, A. N. M. (2018). Secondary Metabolites: Secondary Metabolic Products Consisting of C and H; C, H, and O; N, S, and P Elements; and O/N Heterocycles. In: *Therapeutic Use of Medicinal Plants and their Extracts: Volume 2. Progress in Drug Research*, vol 74. Springer, Cham. https://doi.org/10.1007/978-3-319-92387-1_3.
5. Aryal, S., Baniya, M. K., Danekhu, K., Kunwar, P., Gurung, R., and Koirala, N. (2019). Total phenolic content, flavonoid content and antioxidant potential of wild vegetables from Western Nepal. *Plants*, 8(4): 96. <https://doi.org/10.3390/plants8040096>.
6. Atangana, E., Chiweshe, T. T., and Roberts, H. (2019). Modification of novel chitosan-starch cross-linked derivatives polymers: synthesis and characterization. *Journal of Polymers and the Environment*, 27(5): 979-995. <https://doi.org/10.1007/s10924-019-01407-0>.
7. Bello, A. A., Issa, N., Mawardi, K., and Batch, A. (2025). Antioxidant Activity of Some Apiaceae Plants Wild Distributed in Aleppo, Syria. *South African Journal of Chemical Engineering*, 54: 200-209. <https://doi.org/10.1016/j.sajce.2025.08.003>.
8. Dos Santos, D. C., da Silva Barboza, A., Ribeiro, J. S., Junior, S. A. R., Campos, Â. D., and Lund, R. G. (2022). *Bixa orellana* L.(Achiote, Annatto) as an antimicrobial agent: A scoping review of its efficiency and technological prospecting. *Journal of Ethnopharmacology*, 287: 114961. <https://doi.org/10.1016/j.jep.2021.114961>.
9. Eisenring, M., Best, R. J., Zierden, M. R., Cooper, H. F., Norstrem, M. A., Whitham, T. G., ... and Lindroth, R. L. (2022). Genetic divergence along a climate gradient shapes chemical plasticity of a foundation tree species to both changing climate and herbivore damage. *Global Change Biology*, 28(15): 4684-4700. <https://doi.org/10.1111/gcb.16275>.
10. Eisenring, M., Best, R. J., Zierden, M. R., Cooper, H. F., Norstrem, M. A., Whitham, T. G., ... and Lindroth, R. L. (2022). Genetic divergence along a climate gradient shapes chemical plasticity of a foundation tree species to both changing climate and herbivore damage. *Global Change Biology*, 28(15): 4684-4700. <https://doi.org/10.1111/gcb.16275>.
11. Elshikh, M., Ahmed, S., Funston, S., Dunlop, P., McGaw, M., Marchant, R., and Banat, I. M. (2016). Resazurin-based 96-well plate microdilution method for the determination of minimum inhibitory concentration of biosurfactants. *Biotechnology letters*, 38(6): 1015-1019. <https://doi.org/10.1007/s10529-016-2079-2>.

12. European Food Safety Authority. (2009). The potential risks arising from nanoscience and nanotechnologies on food and feed safety. EFSA Journal, 958: 1-<https://doi.org/10.2903/j.efsa.2009.958>.

13. Franklin, V. A., Hi, E. M. B., Wadt, N. S., and Bach, E. E. (2023). Aqueous extract from urucum (*Bixa orellana* L.): antimicrobial, antioxidant, and healing activity. Porto biomedical journal, 8(1): e183. DOI: 10.1097/j.pbj.0000000000000183.

14. Ghasemi Pirbalouti, A., Siahpoosh, A., Setayesh, M., and Craker, L. (2014). Antioxidant activity, total phenolic and flavonoid contents of some medicinal and aromatic plants used as herbal teas and condiments in Iran. Journal of medicinal food, 17(10): 1151-1157. <https://doi.org/10.1089/jmf.2013.0057>.

15. Handayani, I., Septiana, A. T., and Sustriawan, B. (2024). Natural pigments and antioxidants properties of annatto extract at various pH of distilled water solvent and extraction times. Food Research, 8(2): 489-494. [https://doi.org/10.26656/fr.2017.8\(2\).394](https://doi.org/10.26656/fr.2017.8(2).394).

16. Hlatshwayo, S.; Thembane, N.; Krishna, S. B. N.; Gqaleni, N. and Ngcobo, M. (2025). Extraction and Processing of Bioactive Phytoconstituents from Widely Used South African Medicinal Plants for the Preparation of Effective Traditional Herbal Medicine Products: A Narrative Review. Plants. 14 (206): 1-32. <https://doi.org/10.3390/plants14020206>

17. Hochma, E., Yarmolinsky, L., Khalfin, B., Nisnevitch, M., Ben-Shabat, S., and Nakonechny, F. (2021). Antimicrobial effect of phytochemicals from edible plants. Processes, 9(11): 2089. <https://doi.org/10.3390/pr9112089>.

18. Hodoroaba, V. D. (2020). Energy-dispersive X-ray spectroscopy (EDS). In Characterization of nanoparticles, 397-417. <https://doi.org/10.1016/B978-0-12-814182-3.00021-3>.

19. Jassim, E. H. (2022). Characterization of chitosan nanoparticles coated with *syzygium aromaticum* extract and evaluation their inhibitory activity against *Klebsiella pneumoniae*. MSc Thesis, University of Baghdad, Iraq.

20. Karmakar, U. K., Sultana, S., Nishi, S., Biswas, N. N., Hossain, L., and Sheikh, S. (2018). Antioxidant, analgesic, antimicrobial, and anthelmintic activity of the dried seeds of *Bixa orellana* (L). International Journal of Pharmacy, 8(1): 150-163.

21. Kaur, P., Choudhary, A., and Thakur, R. (2013). Synthesis of chitosan-silver nanocomposites and their antibacterial activity. Int Journal Scientific Engineering Research, 4(4): 869.

22. Khalid, M. A., Niaz, B., Saeed, F., Afzaal, M., Islam, F., Hussain, M., ... and Al-Farga, A. (2022). Edible coatings for enhancing safety and quality attributes of fresh produce: A comprehensive review. International Journal Food Properties 25(1): 1817-1847. <https://doi.org/10.1080/10942912.2022.2107005>.

23. Li, L. H., Deng, J. C., Deng, H. R., Liu, Z. L., and Xin, L. (2010). Synthesis and characterization of chitosan/ZnO nanoparticle composite membranes. Carbohydrate research, 345(8): 994-998. <https://doi.org/10.1016/j.carres.2010.03.019>.

24. Liao, W., Badri, W., Dumas, E., Ghnimi, S., Elaissari, A., Saurel, R., and Gharsallaoui, A. (2021). Nanoencapsulation of essential oils as natural food antimicrobial agents: An overview. *Applied Sciences*, 11(13): 5778. <https://doi.org/10.3390/app11135778>.

25. Litvin, V. A., and Minaev, B. F. (2013). Spectroscopy study of silver nanoparticles fabrication using synthetic humic substances and their antimicrobial activity. *Spectrochimica Acta Part A: Molecular and Biomolecular Spectroscopy*, 108: 115-122. <https://doi.org/10.1016/j.saa.2013.01.049>.

26. López-Meneses, A. K., Plascencia-Jatomea, M., Lizardi-Mendoza, J., Fernández-Quiroz, D., Rodríguez-Félix, F., Mouríño-Pérez, R. R., and Cortez-Rocha, M. O. (2018). *Schinus molle* L. essential oil-loaded chitosan nanoparticles: Preparation, characterization, antifungal and anti-aflatoxigenic properties. *Lwt*, 96: 597-603. <https://doi.org/10.1016/j.lwt.2018.06.013>.

27. Mafe, A. N., Edo, G. I., Makia, R. S., Joshua, O. A., Akpoghelie, P. O., Gaaz, T. S., ... and Umar, H. (2024). A review on food spoilage mechanisms, food borne diseases and commercial aspects of food preservation and processing. *Food Chemistry Advances*, 5: 100852. <https://doi.org/10.1016/j.focha.2024.100852>.

28. Nasti, A., Zaki, N. M., De Leonardis, P., Ungphaiboon, S., Sansongsak, P., Rimoli, M. G., and Tirelli, N. (2009). Chitosan/TPP and chitosan/TPP-hyaluronic acid nanoparticles: systematic optimisation of the preparative process and preliminary biological evaluation. *Pharmaceutical research*, 26(8): 1918-1930. <https://doi.org/10.1007/s11095-009-9908-0>.

29. Ntohogian, S.; Gavriliadou, V.; Christodoulou, E.; Nanaki, S.; Lykidou, S.; Naidis, P.; Mischopoulou, L.; Barmpalexis, P.; Nikolaidis, N. and Bikaris, D. N. (2018). Chitosan Nanoparticles with Encapsulated Natural and UF-Purified Annatto and Saffron for the Preparation of UV Protective Cosmetic Emulsions *Molecules* 23 (2107);1-19. doi:10.3390/molecules23092107

30. Oh, J. W., Chun, S. C., and Chandrasekaran, M. (2019). Preparation and in vitro characterization of chitosan nanoparticles and their broad-spectrum antifungal action compared to antibacterial activities against phytopathogens of tomato. *Agronomy*, 9(1): 21. <https://doi.org/10.3390/agronomy9010021>.

31. Ojha, S., Sett, A., and Bora, U. (2017). Green synthesis of silver nanoparticles by *Ricinus communis* var. *carmencita* leaf extract and its antibacterial study. *Advances in Natural Sciences: Nanoscience and Nanotechnology*, 8(3): 035009. DOI: 10.1088/2043-6254/aa724b.

32. Singh, M., Thippareddi, H., Wang, L., and Balamurugan, S. (2019). Meat and poultry. *Food microbiology: fundamentals and frontiers*, 125-177. <https://doi.org/10.1128/9781555819972.ch6>.

33. Taham, T., Cabral, F. A., and Barrozo, M. A. (2015). Extraction of bixin from annatto seeds using combined technologies. *The Journal of Supercritical Fluids*, 100: 175-183. <https://doi.org/10.1016/j.supflu.2015.02.006>.

34. Viuda-Martos, M., Ciro-Gómez, G. L., Ruiz-Navajas, Y., Zapata-Montoya, J. E., Sendra, E., Pérez-Álvarez, J. A., and Fernández-López, J. (2012). In vitro Antioxidant and antibacterial activities of Extracts from Annatto (*Bixa orellana*

L.) Leaves and Seeds. *Journal of Food Safety*, 32(4): 399-406. <https://doi.org/10.1111/j.1745-4565.2012.00393.x>.

35. Wenli, D., Zirong, X., Xinyan, H., Yinglei, X., and Zhiguo, M. (2008). Preparation, characterization and adsorption properties of chitosan nanoparticles for eosin Y as a model anionic dye. *Journal of Hazardous Materials*, 153(1-2): 152-156. <https://doi.org/10.1016/j.jhazmat.2007.08.040>.

36. Willems, T., De Mol, M. L., De Bruycker, A., De Maeseneire, S. L., and Soetaert, W. K. (2020). Alkaloids from marine fungi: Promising antimicrobials. *Antibiotics*, 9(6): 340. <https://doi.org/10.3390/antibiotics9060340>.

37. Yolmeh, M., Najafi, M. B. H., Farhoosh, R., and Salehi, F. (2014). Modeling of antibacterial activity of annatto dye on *Escherichia coli* in mayonnaise. *Food Bioscience*, 8: 8-13. <https://doi.org/10.1016/j.fbio.2014.09.001>.

38. Zeng, W. C., He, Q., Sun, Q., Zhong, K., and Gao, H. (2012). Antibacterial activity of water-soluble extract from pine needles of *Cedrus deodara*. *International journal of food microbiology*, 153(1-2): 78-84. <https://doi.org/10.1016/j.ijfoodmicro.2011.10.019>.